

Use of Modified Lignocellulosic Butanol Residue in Phenol-Resorcinol-Formaldehyde Polymers

Juan Liu,^a Zuxin Zhang,^a Riqing Chen,^a Yuzhi Xu,^a Chupeng Wang,^a and Fuxiang Chu^{b,*}

Lignocellulosic butanol residue (BR), obtained as the by-product of lignocellulosic butanol production, was used for the preparation of lignin-based phenol-resorcinol-formaldehyde resins (LPRFRs) by condensation polymerization. The lignin was first phenolated under sodium hydroxide catalysis at 90 to 92 °C at various phenolation times (1.0 to 4.0 h). The structural differences between BR and phenolated BR (PBR) were studied using Fourier transform infrared (FT-IR) spectroscopy, ultraviolet (UV) spectroscopy, thermogravimetric analysis (TGA), and gel permeation chromatography (GPC). The BR phenolated for 3.0 h had high phenol hydroxyl content, low molecular weight, and good thermal stability. The LPRFRs with 30 wt.% BR had the lowest free formaldehyde and phenol. With the substitution of BR for phenol, the hydrophilicity of LPRFRs increased. In addition, the mechanical, fragility, thermal properties, and morphology of lignin-phenol-resorcinol-formaldehyde foams (LPRFFs) were also investigated. The LPRFFs had excellent comprehensive properties when 30 wt.% PBR was substituted for phenol. These experimental findings could provide a new avenue for further study and application of bio-phenol-resorcinol foams.

Keywords: *Lignin phenolation; Lignin-based phenol-resorcinol-formaldehyde resins; Foams; Mechanical Properties; Thermal stability*

Contact information: *a: National Engineering Laboratory for Biomass Chemical Utilization, Key and Open Laboratory on Forest Chemical Engineering, Key Laboratory of Biomass Energy and Material, Institute of Chemical Industry of Forestry Products, CAF210042, Nanjing, Jiangsu, China; b: Chinese Academy of Forestry 100091, Beijing, China; *Corresponding authors: chufxg@163.com; wangcpg@163.com*

INTRODUCTION

Phenolic foams are widely used because of their advantageous features, such as fire-resistance, dimensional stability, and chemical corrosion resistance, compared with other polymeric foams (Ma *et al.* 2013; Del Saz-Orozco *et al.* 2015). Phenolic foams are mostly produced with petroleum-based phenol and formaldehyde chemicals (Pilato 2013; Ding *et al.* 2015). However, petroleum-based phenol possesses strong toxicity and is resistant to biochemical degradation, which seriously threatens the ecological environment and human health. As the second most abundant biopolymer, lignin contains rich functional groups such as phenolic hydroxyl groups, benzene rings, and ether linkages, and plays a significant role as an alternative source for phenolics (El-Saied *et al.* 1984; Cetin and Özmen 2002; Wang *et al.* 2009; Grishechko *et al.* 2013). The incorporation of lignin units in phenolic foams not only reduces the production cost and environment pollution, but also promotes the development of the biomaterial industry.

However, lignin has lower chemical reactivity than simple phenol because of its high molecular weight and crosslinked structure, which hinders effective condensation reactions (Li *et al.* 2008; Podschun *et al.* 2015). Lignin is primarily modified chemically

by phenolation, methylolation, and demethylation (Funaoka *et al.* 1995; Filley *et al.* 2002; Malutan *et al.* 2007) reactions. Among them, phenolation is considered the most promising modification method because of its simple process and satisfactory results (Zhao *et al.* 2016). There are many publications on lignin phenolation reactions and the preparation of sustainable lignin-based phenol foams. The phenolation modification of lignin is usually achieved using acid catalysts such as oxalic acid, hydrochloric acid, and sulfuric acid (El-Saied *et al.* 1984; Alonso *et al.* 2005; Ma *et al.* 2011; Zhou *et al.* 2015). However, the synthesis reaction of thermoset phenolic resin for foaming is generally catalyzed by alkalis. Therefore, the reaction system should be adjusted to a basic medium, which would waste energy produced *via* neutralizing acid catalysis (Zhao *et al.* 2016). The partial replacement of petroleum-based phenol by phenolated lignocellulosic butanol residue (PBR) to prepare lignin-based-phenol-resorcinol-formaldehyde resins (LPRFRs) catalyzed by alkalis has rarely been reported.

As the by-product of lignocellulosic butanol production, lignocellulosic butanol residue (BR) was used for the preparation of bio-phenolic foams. The present work aimed to phenolate lignocellulosic butanol residue (BR) in the presence of a basic catalyst to improve the reactivity of BR and to produce LPRFRs and lignin-based-phenol-resorcinol-formaldehyde foams materials (LPRFFs). The effects of phenolation time on BR were studied using analytical techniques, such as Fourier transform infrared (FT-IR) spectroscopy, ultraviolet (UV) spectroscopy, gel permeation chromatography (GPC), and thermogravimetric analysis (TGA). The physicochemical and wetting properties of LPRFRs under different phenolation times and BR replacement percentages of phenol were analyzed. In addition, the mechanical and thermal properties as well as the morphology of LPRFFs were also studied.

EXPERIMENTAL

Materials

The BR sample (polysaccharide 1.5 wt.%, ash 3.9 wt.%, and holocellulose 11.9 wt.%) was provided by Songyuan Guanghe Energy Co., Ltd (Songyuan, China). The chemicals phenol, 37 wt.% formaldehyde aqueous solution, paraformaldehyde, petroleum ether, and sodium hydroxide were obtained from Nanjing Chemical Reagent, Ltd (Nanjing, China). Resorcinol and polysorbate 80 were supplied from Sinopharm Chemical Reagent Co., Ltd (Shanghai, China). All reagents used for the chemical analysis were of analytical grade.

Methods

Phenolation of BR and synthesis of LPRFRs

Phenol (300 g), BR (80 g), and 30 wt.% NaOH solution (38 g) were mixed in a 1000-mL flask. The phenolation of BR was carried out at 90 to 92 °C at various reaction times (1.0, 2.0, 3.0, and 4.0 h) to explore the optimum phenolation time. The replacement percentage of phenol in BR was increased from 0 to 50 wt.% while keeping the optimum phenolation time of 3 h. The molar ratio of formaldehyde to phenol, BR, and resorcinol was 2.0:1.0 (Zhang *et al.* 2013). First, the formaldehyde aqueous solution was added into a mixture of phenol and PBR. After reacting at 88 °C for 0.5 h, the paraformaldehyde was charged into the flask every 15 min. Then, the flask was cooled down to 70 °C and resorcinol was added to the system. It was then allowed to react for

approximately 40 min. Finally, the synthesized resins were cooled down to room temperature quickly and the pH of the prepared LPRFRs was adjusted to 7.0 with formic acid. The synthesized LPRFRs contained high-solid resins with 70 to 80 wt.% solid contents.

Preparation of LPRFFs

Approximately 100 g of LPRFRs and 5 g of surfactant (polysorbate 80) were first added into a mixer, and the contents were stirred and mixed well by a high-speed mixer at room temperature. Second, 8 g of blowing agent (petroleum ether) was added to the mixer and allowed to mix quickly to prevent evaporation. Then, 20 g of complex acid curing agent (wt/wt: sulfuric acid/phosphoric acid/*p*-toluenesulfonic acid/water = 2.0:1.0:1.5:2.5) was put into the mixer. After beating well, the mixture was poured into a mold and cured at 70 °C for 50 min. The density of prepared foams was approximately 52 kg/m³.

Characterization of BR and PBR

FT-IR analysis

The BR and PBR samples were treated with diethyl ether and HCl solution and dehydrated at 40 °C for 48 h with a vacuum drying oven according to a literature procedure (Gordobil *et al.* 2014). The FT-IR analysis was carried out with a Nicolet iS10 FT-IR spectrometer (Thermo Fisher Scientific, USA). The spectrum was acquired from a range of 500 to 4000 cm⁻¹.

Ultraviolet (UV) analysis

The phenolic hydroxyl contents of BR and PBR samples were obtained by the ultraviolet differential spectra method. The UV-spectra and absorbances of BR and PBR were obtained by adding 2 mL of lignin-dioxane-water solution (3 g/L in 9:1 v/v dioxane and water) to 48 mL of NaOH solution (0.2 M) or phosphate buffer at pH 6.0 using a UV-1800PC spectrophotometer (Mapada, China) (Mancera *et al.* 2011; Liu 1996).

GPC analysis

The weight average molecular weight (M_w), number average molecular weight (M_n), and polydispersity index (M_w/M_n) of BR and PBR samples were evaluated using a gel permeation chromatographic (Malvern, UK) analyzer equipped with a 1122 binary pump and a 3580 refractive index detector.

THF was used as a mobile phase at the flow rate of 1 mL/min, and polystyrene standards were used to obtain the calibration curve. The samples of BR and PBR were first treated with pyridine and then with acetic anhydride in the volume ratio of 1:1 to increase their solubility in organic solvents, as per reported methods (Tejado *et al.* 2007; El Hage *et al.* 2009).

TGA analysis

The thermal stability and degradation of BR, PBR, and LRPFFs were studied using a thermogravimetric analyzer. Thermogravimetric (TG) measurements were performed using a Netzsch (Germany) STA 409 apparatus. Approximately 4 to 5 mg of samples was scanned from 35 to 900 °C at a heating rate of 10 °C/min under nitrogen gas at a flow rate of 0.02 L/min.

Characterization of LPRFRs

Physicochemical properties of LPRFRs

The viscosity, solids content, free phenol, and free formaldehyde contents were tested in accordance with the ASTM standard D1084 (2008), ASTM standard D4426 (2001), and GB/T 14074 (2006), respectively (Zhang *et al.* 2013a).

Contact angle measurements

The LPRFRs with 0, 30, and 50 wt.% BR substitution were heated at 60 °C for 5 h and then at 100 °C for 3 h to obtain resin films. The sessile drop method was used to measure the contact angle of resin films using a DSA100 contact angle analyzer (Kruss, Germany) at 15 °C. To obtain the surface free energy, three liquids water, ethylene glycol, and glycerol were used.

Characterization of LPRFFs

Mechanical properties of LPRFFs

Compressive and flexural strengths were tested with a CMT4000 universal testing machine (Shenzhen, China) according to Chinese National Standards ISO 844 (2004) and ISO 1209-1 (2004), respectively.

Fragility properties of LPRFFs

Fragility reflected the mechanical properties of LRPFFs indirectly. The LRPFFs prepared were cut into 12 cubes (with dimensions of 25×25×25 mm³) for testing according to ISO 6187 (2001).

TGA measurements of LPRFFs

A thermogravimetric analyzer (TGA) was used to study the thermal stability and degradation of LRPFFs. The samples used for analysis (4 to 5 mg) were scanned from 35 to 900 °C at a heating rate of 10 °C/min under a nitrogen atmosphere (0.02 L/min).

Morphology of LPRFFs

The morphological structures of LRPFFs were evaluated by scanning electron microscopy (SEM, S-3400N, Hitachi Co., Japan). The fracture surface of samples was first gold-coated (E-1010 ion sputter, Hitachi Co., Japan) with a conductive layer to avoid electrostatic charging during the experimental testing process. The accelerating voltage was 15 kV, and the working distance was 28.2 mm.

RESULTS AND DISCUSSION

Characterization of BR and PBR

FT-IR spectra analysis

FT-IR spectra of BR and PBR samples are shown in Fig. 1 in the range from 600 to 4000 cm⁻¹. The absorption bands at 3332 cm⁻¹ were attributed to O–H stretching vibrations (both phenolic OH and aliphatic OH). Bands at 1509 cm⁻¹ were attributed to C–C stretching vibration of aromatic skeleton. The peaks at 1213 cm⁻¹ were due to the C–O stretching vibration of phenolic C–OH and ether linkages; meanwhile, the peaks at 1030 cm⁻¹ were for the C–H deformation vibration of primary hydroxyl and ether groups. In addition, the bands at 755 cm⁻¹ were due to C–H (Ar) in-plane deformation vibration

of guaiacyl lignin (G-lignin), and the bands at 692 cm^{-1} were assigned to the presence of C–H (Ar) out-of-plane deformation vibration of mono-substituted benzene ring structure.

There were differences between the IR spectra of BR and PBR with different phenolation times, which indicated the structural change between them. With an increase in phenolation time, the band intensities at 3332 cm^{-1} increased in PBR, indicating that there was an increase of O–H contents after phenolation. And the peaks at 1509 and 1213 cm^{-1} became sharper and intense, which indicated that the phenolic modification of BR could improve the content of phenolic OH. The intensity of PBR bands located at 755 and 692 cm^{-1} also increased markedly. That was due to the nucleophilic substitution between *ortho* or *para* hydrogen of phenol and the α -position of the phenylpropane units of lignin were substituted by hydroxyl groups (Doherty *et al.* 2011; Zhao *et al.* 2016). However, the peak of 3.0 h PBR at 1030 cm^{-1} was weaker than that of 4.0 h PBR, which arose from the condensation reaction between hydroxyl groups of 4.0 h PBR (Matsushita *et al.* 2009). Phenolic OH serves as an important functional group in preparing the LPRFRs by activating the free ring positions to make them reactive with formaldehyde. It was obviously that the phenolic OH contents of BR were improved by phenolation treatment, which provided an effective approach to make the best use of lignocellulosic butanol residue to prepare LPRFRs.

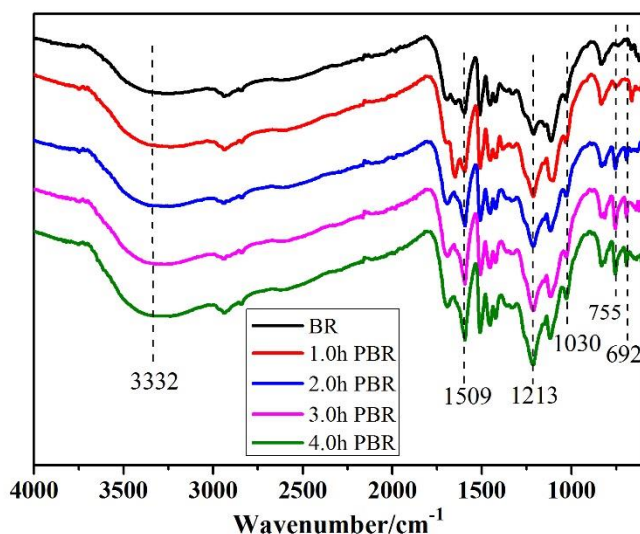


Fig. 1. FT-IR spectra of BR and PBR samples with different phenolation times

Ultraviolet differential analysis

Phenolic hydroxyl content could be obtained by UV-differential spectral analysis at 298 and 356 nm (Dos-Santos *et al.* 2010). The absorbance, extinction coefficient, and phenol hydroxyl content of BR phenolated at different reaction time are presented in Table 1. It was clearly apparent that the phenolic hydroxyl content first increased and then decreased with phenolation time. The phenolic hydroxyl content of BR before phenolation was 2.91% , and that of PBR phenolated for 3.0 h reached a maximum of 3.36% . However, the phenolic hydroxyl content decreased while BR phenolated for 4.0 h because of the re-polymerization reaction of hydroxyl groups. The BR could be decomposed into low-molecular-weight and highly-reactive fragments during the

phenolation process at high temperature (Matsushita *et al.* 2009), which was also confirmed by the GPC measurement. When the phenolation time was too long at high temperature, the recondensation of reactive fragments and phenol occurred and resulted in low-phenol hydroxyl content and high molecular weight (Saisu *et al.* 2003). These results indicated that the BR phenolated for 3.0 h had the highest activity compared with other BR samples and was more suitable to react with formaldehyde and to prepare LPRFRs.

Table 1. Absorbances and Extinction Coefficients of BR and PBR Samples

Time (h)	Wavelength (nm)	Absorbance	Extinction Coefficient ($L \cdot g^{-1} \cdot cm^{-1}$)	Phenol Hydroxyl Content (%)
0	298	0.318	5.30	2.91
	356	0.217	3.62	
1.0	298	0.323	5.38	2.94
	356	0.216	3.60	
2.0	298	0.330	5.50	3.01
	356	0.221	3.68	
3.0	298	0.366	6.10	3.36
	356	0.254	4.23	
4.0	298	0.298	4.97	2.69
	356	0.190	3.17	

GPC analysis

The BR phenolic modification had an effect on the molecular weights of BR and PBR samples. Table 2 shows the values of weight average molecular weight (M_w), number average molecular weight (M_n), and polydispersity index (M_w/M_n) of BR and PBR phenolated for various times. Among the four phenolated PBR samples, the PBR phenolated for 1 and 2.0 h presented a slightly lower M_w , M_n , and M_w/M_n compared with BR, while the PBR phenolated for 3.0 h had the lowest M_w , M_n , and M_w/M_n and PBR phenolated for 4 h had a slightly higher M_w and M_n than BR. During the phenolation process, the carbon–oxygen bond at α -position of the phenylpropane units of lignin was attacked first by hydroxide ions, resulting in the cleavage of ether linkages. Then, the *ortho* or *para* hydrogen of phenol reacted with lignin. Additionally, the presence of phenol could inhibit the self-condensation of PBR fractions (Brebu and Vasile 2010). However, when the phenolation treatment was more than 3.0 h, the self-condensation of PBR would play a dominant role in phenolation reaction, which would cause M_w , M_n , and M_w/M_n of PBR to become higher. The results suggested that the BR phenolated for 3.0 h was more suitable for condensation with formaldehyde because of less steric hindrance (Zhang *et al.* 2013b).

Table 2. Weight Average (M_w), Number Average (M_n), and Polydispersity Index (M_w/M_n) of BR and PBR Samples

Phenolation Time (h)	M_n	M_w	M_w/M_n
0	2390	4510	1.89
1.0	2250	3750	1.67
2.0	2230	3640	1.63
3.0	1730	2580	1.49
4.0	2610	4710	1.80

Thermal properties

The thermogravimetric (TG) and derivative thermogravimetric (DTG) curves of BR and 3.0 h PBR samples are presented in Fig. 2. The initial degradation temperature ($T_{5\%}$), the 20% weight loss temperature ($T_{20\%}$), the maximum weight loss temperature (T_{\max}), and char residue (at 900 °C) for BR and 3.0 h PBR are shown in Table 3. The decomposition process could be divided into three stages with different molecular weight distributions presented in BR and 3.0 h PBR. The BR and PBR had a small weight loss below 200 °C, attributed to moisture evaporation and the degradation of low-molecular weight organic compounds (Zhang *et al.* 2016). At this stage, the weight loss rate of 3.0 h PBR was a little more than that of the BR sample. However, the initial degradation temperature ($T_{5\%}$) of 3.0 h PBR was much higher than that of BR, with values of 237.6 and 190.2 °C, respectively, which indicated that the phenolation treatment could improve the thermostability of lignin. The second stage, which ranged from approximately 200 to 650 °C, was the main devolatilization process. The weight loss rate of 3.0 h PBR was similar to that of BR. During this process, the demethylation of the dimethoxy-groups led to the conversion of phenols into pyrocatechols, and thus two-oxygen atom products were formed by the cleavage of the methoxy group C–O bonds. In addition, the cleavage of the side chain C–C bond occurred between the aromatic ring and the α-C atom (Demirbas *et al.* 2004; Brebu and Vasile 2010). The third stage took place between 650 and 900 °C, which was attributed to the carbonization process.

As shown in Table 3, the $T_{20\%}$ and T_{\max} of 3.0 h PBR were 361.3 and 379.2 °C, respectively, while those of BR were 328 and 371.3 °C, respectively. Thus, 3.0 h PBR exhibited higher temperatures ($T_{20\%}$ and T_{\max}) than BR, and the content of char residue of 3.0 h PBR and BR at 900 °C were 43.54% and 39.48%, respectively. It can be inferred that the thermal stability of lignin was enhanced by phenolation treatment because the thermal properties of lignin mostly depend on the type of oxygen functional groups in the lignin structure (Brebu and Vasile 2010). During the phenolic reaction process, highly reactive and unstable free radicals were formed by cleavage of the aryl–ether group, which further reacted through rearrangement, electron abstraction, or radical–radical interactions to form products with increased stability (Afifi *et al.* 1989).

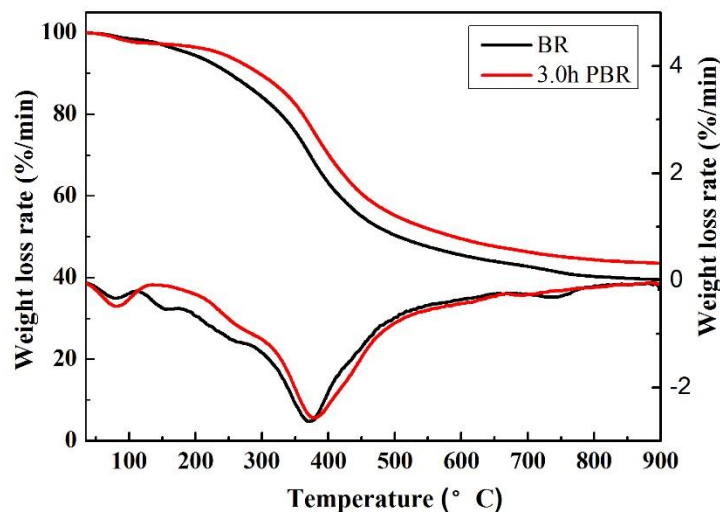


Fig. 2. TG and DGT curves of BR and 3.0 h PBR samples

Table 3. TG Data of BR and 3.0 h PBR Samples

Sample	T _{5%} (°C)	T _{20%} (°C)	T _{max} (°C)	Char Residue (%)
BR	190.2	328.0	371.3	39.48
3.0 h PBR	237.6	361.3	379.2	43.54

Characterization of LPRFRs

Physicochemical properties of LPRFRs

The physicochemical properties of LPRFRs formed at various phenolation times, and the BR replacement percentages of phenol are displayed in Table 4. Free phenol and free formaldehyde contents of the resin without BR were quite low, at 1.85% and 0.22%, respectively. With phenolation time increasing from 0 to 2.0 h, the viscosity, solids content, free phenol, and free formaldehyde contents of LPRFRs that BR replaced with 20 wt.% phenol had little change. The free phenol and free formaldehyde contents of LPRFRs with 3.0 h PBR had minimum values, which was due to the fact that the PBR was more reactive and reacted well with formaldehyde. Viscosity, free phenol, and free formaldehyde contents of LPRFRs with 4.0 h PBR were markedly increased because the PBR re-polymerization occurred and the activity of PBR was decreased. Additionally, the high viscosity hindered the reaction between resorcinol and formaldehyde in the late stage of polymerization, which would increase free formaldehyde content.

With the substitution of BR (phenolated for 3.0 h) for phenol, the viscosity, solids content, free phenol, and free formaldehyde contents of LPRFRs showed an increasing trend because of the lower chemical activity of BR compared with phenol. Also, BR contained some polysaccharide, ash, and holocellulose. When the BR replacement percentage of phenol was higher than 30 wt.%, the free phenol and free formaldehyde contents were too high to affect human health. When BR was displaced 50 wt.% phenol, the high viscosity observed would seriously affect the foaming behavior and make blending LPRFRs with addition agents (surfactant, foaming agent, and curing agent) difficult. Overall, the optimum phenolation time was 3.0 h and the maximum BR replacement percentage of phenol was 30 wt.%.

Table 4. Effects of Reaction Time on Physicochemical Properties of LPRFRs

Time (h)	BR (wt.%)	Viscosity (mPa)	Solid Content (%)	Free Phenol (%)	Free Formaldehyde (%)
0	20	5000	74.5	2.40	0.31
1.0	20	5300	74.6	2.32	0.30
2.0	20	5400	74.5	2.39	0.30
3.0	20	5800	75.4	2.08	0.29
4.0	20	8100	73.8	3.41	0.41
3.0	10	4600	73.4	1.93	0.24
3.0	30	7800	74.1	2.35	0.31
3.0	40	34000	73.1	3.36	0.66
3.0	50	58900	74.0	5.86	1.40
0	0	4100	75.3	1.85	0.22

Contact angle measurements

Contact angle and surface components of LPRFRs with 0, 30, and 50 wt.% BR are shown in Table 5. With the substitution of BR for phenol, the contact angle to water and ethylene glycol of LPRFRs films decreased, while that to glycerol was increased, and the surface free energy was increased. This change in trend was due to different chemical properties of the used liquids and the hydrophilic groups present in LPRFRs. The phenolated BR had high hydroxyl content and the C3 side chain of BR had higher Lifshitz–van der Waals component than the methylene group (Matsushita *et al.* 2006). Therefore, the wettability on the surface of LPRFRs films with BR was better than PRFRs.

Table 5. Contact Angle and Surface Components of LPRFRs with 0, 30, and 50 wt.% BR

BR (wt.%)	Contact Angle (°)			Surface Components (mN·m ⁻¹)				
	Water	Ethylene Glycol	Glycerol	γ	γ^{LW}	γ^{AB}	γ^+	γ^-
0	73.58 (0.58)	50.00 (0.39)	60.75 (0.61)	58.78	56.09	2.69	1.35	1.35
30	51.49 (0.39)	39.21 (0.37)	66.28 (0.20)	67.10	55.56	11.54	5.77	5.77
50	50.49 (2.07)	36.40 (1.83)	65.01 (1.11)	69.10	57.73	11.37	5.69	5.69

γ , the surface free energy; γ^{LW} , Lifshitz–van der Waals component; γ^{AB} , Lewis acid-base component; γ^+ and γ^- represent the electron-acceptor and electron-donor parameters of γ , respectively

Performance Analysis of LPRFFs

Mechanical properties

The effects of phenolation time and BR replacement percentages of phenol on the mechanical properties of LPRFFs had been studied. The compressive and flexural strengths of foam samples are shown in Fig. 3. When the BR replacement percentage of phenol was kept constant at 20 wt.% level, the compressive strength, and flexural strength of LPRFFs were increased first and then decreased dramatically with the increase of phenolation time. The LPRFFs prepared with 3.0 h PBR showed good mechanical performance, whilst the mechanical properties of LPRFFs with 4 h PBR performed poorly, which was due to the re-polymerization of BR fractions and the low reactivity of LPRFRs. Therefore, the best mechanical properties were obtained for the 3.0 h PBR modified LPRFFs samples. The compressive strength and flexural strength for LPRFFs with 3 h PBR were 163.6 and 254.5 kPa, respectively. For unphenolated LPRFFs the corresponding values were 138.1 and 221.8 kPa, with an increase of 18.5% and 14.7% compared to LPRFFs with BR.

Then, holding the phenolation time of BR at 3.0 h, the BR replacement of phenol in the range of 0 wt.% to 40 wt.% was studied. As shown in Fig. 3(b), the compressive strength and flexural strength of LPRFFs increased with the replacement of phenol and decreased when the BR replaced phenol was over 30 wt.%. The compressive strength and flexural strength of PRFFs without BR were 128.1 and 210.5 kPa, respectively and that of LPRFFs with 30 wt.% PBR substitution were 181.6 and 261.6 kPa. The strengths for LPRFFs with 30 wt.% BR were increased by 41.8% and 24.3% relative to PRFFs. When phenol was replaced 40 wt.%, the compressive strength and flexural strength of LPRFFs

were decreased by 11.3% and 8.7%, respectively. Therefore, the LPRFFs with BR 30 wt.% substitution had the best mechanical properties. The higher replacement percentages would decrease the mechanical properties of LPRFFs because large amount of BR would result in low reactivity and curing rate, and high viscosity of LPRFRs, which affected the mechanical properties of LPRFFs.

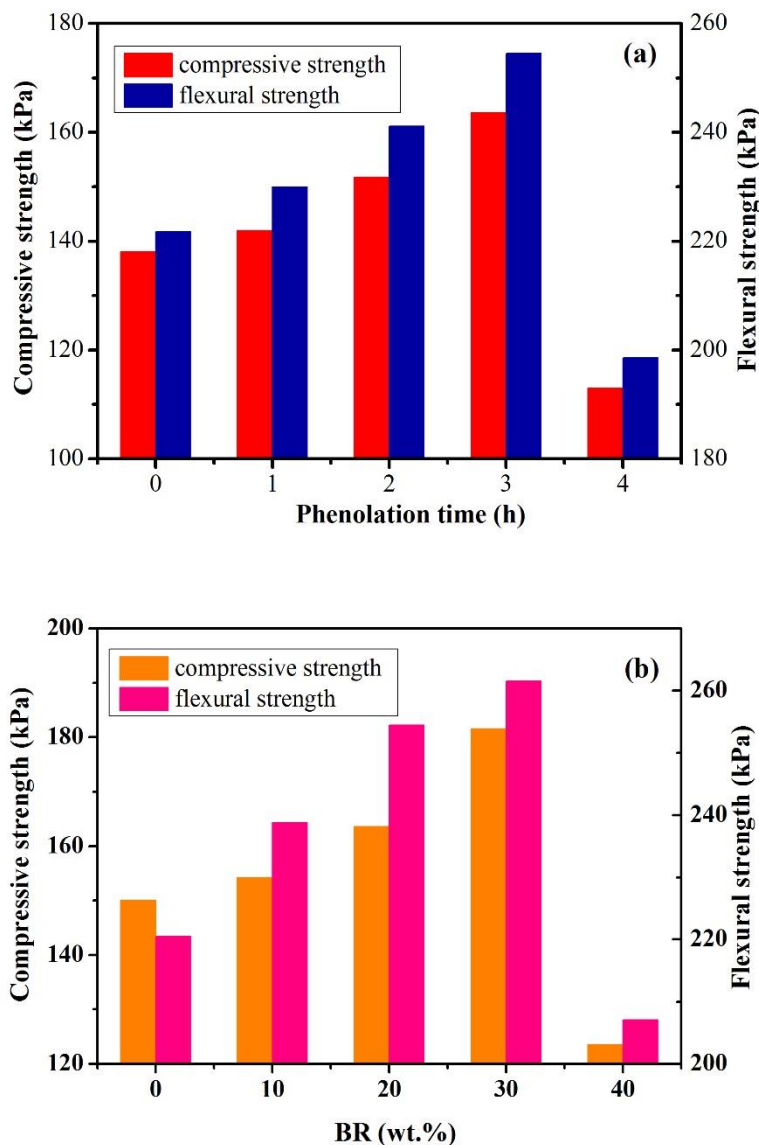


Fig. 3. Effects of (a) phenolation time and (b) BR replacement percentage of phenol on the mechanical properties of LPRFFs

Fragility of LRPFFs

The effects of phenolation time and BR replacement percentages of phenol on the fragility of LPRFFs are depicted in Fig. 4. As shown in Fig. 4(a), the phenolation time could affect the fragility of LPRFFs. The fragility of LPRFFs with BR was 24.3% and that of LPRFFs modified with 3.0 h PBR was 19.4%, which showed a decrease of 20.1%. This result was an indication that extending the phenolation time appropriately could

improve the materials' fragility, and LPRFFs modified with 3.0 h PBR possessed optimum property. As shown in Fig. 4(b), with the replacement percentage increasing from 0 wt.% to 30 wt.%, the fragility of LPRFFs was decreased first, and then increased when BR was replaced with 40 wt.% phenol. The change in trend indicated that the LPRFFs had the best properties with BR replacement percentage at 30 wt.% level. The fragility of the foam matched to its mechanical properties.

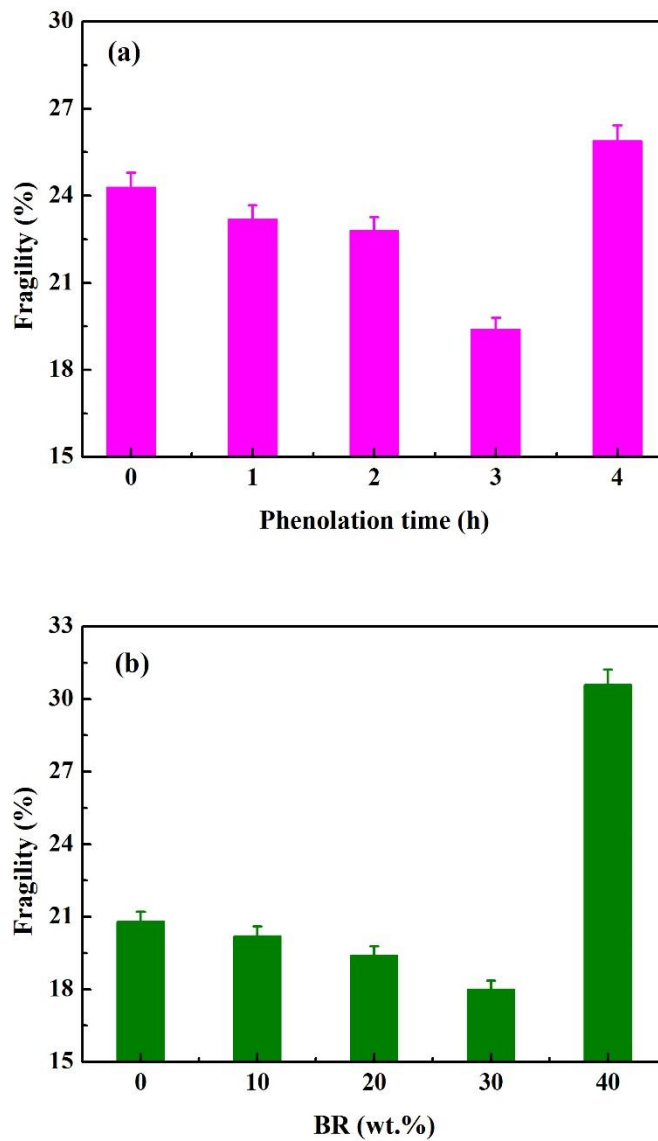


Fig. 4. Effects of (a) phenolation time and (b) BR replacement percentages of phenol on fragility of LPRFFs

Thermal behavior of LPRFFs

The thermograms and the thermal parameters for LPRFFs with 0, 10, 20, 30, and 40 wt.% BR substitutions are shown in Fig. 5. The thermograms for LPRFFs were quite similar to PRFFs and showed four steps of thermal degradation. In the first step (35 to 150 °C), the weight loss was due to phenol, formaldehyde, and moisture losses (Del Saz-Orozco *et al.* 2015). The weight loss in the second step (150 to 220 °C) was due to the

moisture formed by condensation reaction of hydroxyl functional groups including hydroxymethyl group and phenolic hydroxyl (Lee *et al.* 2012) groups. In the third stage (220 to 360 °C), the mass loss observed was attributed to the decomposition of polymer chains, as well as the formation and release of water and formaldehyde moieties. The T_{max} of LPRFFs was lower than that of PRFFs and that of LPRFFs decreased obviously with the increase of BR replacement rate, which are indicated in Fig. 5(b). It was shown that the LPRFFs had lower thermal stability than PRFFs in this stage and the more percentages of BR incorporated into the PRFRs, lowers the thermal stability of LPRFRs. The fourth stage ranged from 360 to 900 °C which was attributed to the degradation of BR and the formation of carbonaceous char.

As shown in Fig. 5(c), $T_{10\%}$ for PRFFs was found at 242.6 °C, whereas for LPRFFs with 20 wt.% BR substitution the $T_{10\%}$ was at 168.3 °C, and that with 40 wt.% BR substitution was at 203.0 °C. With the increase of BR replacement rate, the $T_{10\%}$ of LPRFFs was decreased and then increased when the BR replacement rate was more than 20 wt.%. This might be because of the presence of excess BR, which affected the thermal degradation of LPRFRs within 250 °C and improved the thermal stability. And as shown in Fig. 5(d), the Ash_{900°C} of PRFFs was 48.55%, for LPRFFs with 20 wt.% BR it was 41.09%, and with 40 wt.% BR it was 42.33%, respectively. The Ash_{900°C} content was reduced significantly with the incorporation of BR into PRFFs. Thus, the LPRFRs had lower thermal stability than PRFRs with BR incorporated into the PRFRs.

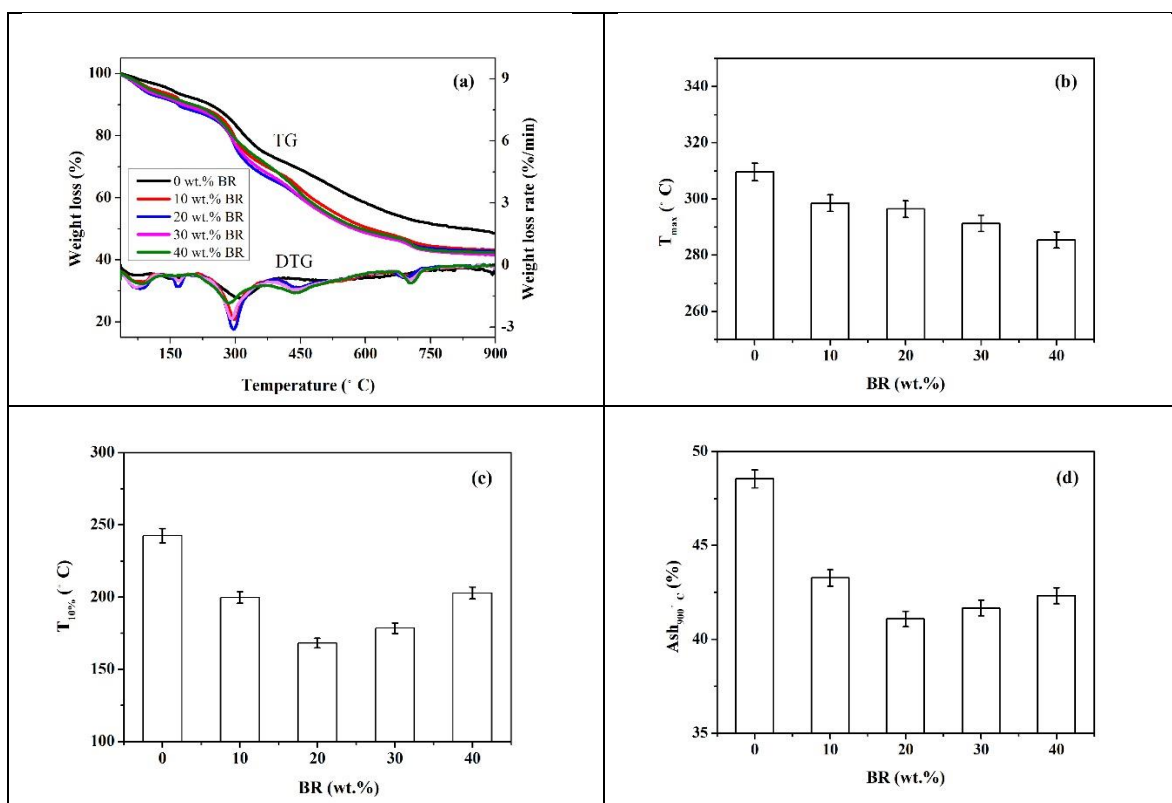


Fig. 5. Thermograms and thermal parameters for LPRFFs with 0, 10, 20, 30, and 40 wt.% BR: (a) thermograms; (b) T_{max} (°C); (c) $T_{10\%}$ (°C); and (d) ash at 900 °C (%)

Morphology of LRPFFs

Figure 6 represents the morphologies of LPRFFs in various phenolation times and BR replacement percentages of phenol. The LPRFFs exhibited obvious spherical shape at

150X magnification. It could be observed that the cell diameter of LPRFFs was small, cell structure was excellent, and the cells distributed well when the foams were produced with LPRFRs modified with 20 wt.% BR that phenolated for 3.0 h. But the cell size of LPRFFs with 20 wt.% BR phenolated for 4.0 h was bigger and not uniform because of the high viscosity of LPRFRs modified with 4.0 h PBR went against bubble formation. It could be also observed that LRPFFs had good cell structure when the BR was phenolated for 3.0 h and the replacement percentage was at 30 wt.% level. And LRPFFs modified with 40 wt.% PBR had big and uniform cell structure because of the excess BR present which would affect its reactivity and viscosity.

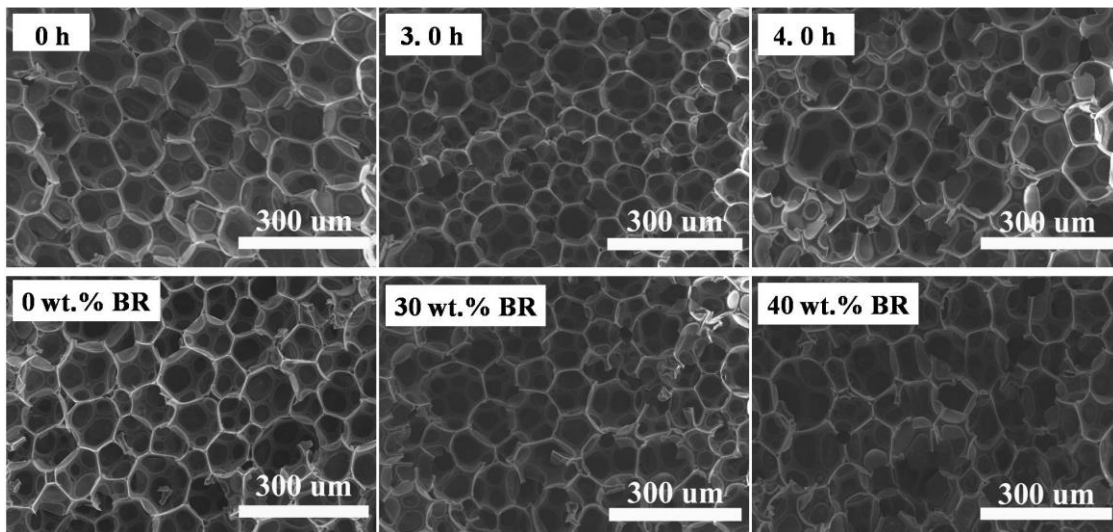


Fig. 6. SEM images for LPRFFs with different phenolation time (0, 3.0, and 4.0 h) and BR replacement percentages (0, 30, and 40 wt.%) of phenol

CONCLUSIONS

In this work, BR was phenolated under different reaction times to increase its chemical reactivity in the presence of sodium hydroxide solution. The phenolated BR was then used to replace phenol to prepare LPRFRs and LPRFFs.

1. The BR phenolated for 3.0 h had lowest molecular weight and best thermal stability. And the phenolic hydroxyl content of BR was increased to 3.36% by phenolation treatment.
2. The LPRFRs with 30 wt.% BR that was phenolated for 3 h had low free formaldehyde and free phenol contents, which were 0.29% and 2.08%, respectively. With the substitution of BR for phenol, the contact angles of LPRFRs decreased and its surface free energy increased because of the increase of hydrophilic groups.
3. The greatest mechanical properties for the modified phenolic foams were obtained by replacing with 30 wt.% phenol, and its compressive and flexural strengths increased by 41.8% and 24.3%, respectively. As a whole, LPRFFs with 30 wt.% BR that phenolated for 3 h had the best features.

ACKNOWLEDGMENT

This work was supported by the Fundamental Research Funds for the Central Non-profit Research Institution of CAF, Grant. No. CAFYBB2016ZX002 and the National Natural Science Fund of China, Grant. No. 31200448.

REFERENCES CITED

- Afifi, A., Hindermann, J., Chornet, E., and Overend, R. (1989). "The cleavage of the aryl OCH₃ bond using anisole as a model compound," *Fuel* 68(4), 498-504. DOI: 10.1016/0016-2361(89)90273-1
- Alonso, M. V., Oliet, M., Rodríguez, F., García, J., Gilarranz, M. A., and Rodríguez, J. J. (2005). "Modification of ammonium lignosulfonate by phenolation for use in phenolic resins," *Bioresour. Technol.* 96(9), 1013-1018. DOI: 10.1016/j.biortech.2004.09.009.
- ASTM standard D1084 (2008). "Standard test methods for viscosity of adhesives," American Society for Testing and Materials, Philadelphia, PA, America.
- ASTM standard D4426 (2001). "Standard test method for determination of percent nonvolatile content of liquid phenolic resins used for wood laminating," American Society for Testing and Materials, Philadelphia, PA, America.
- Brebu, M., and Vasile, C. (2010). "Thermal degradation of lignin—A review," *Cellul. Chem. Technol.* 44(9), 353-363.
- Cetin, N. S., and Özmen, N. (2002). "Use of organosolv lignin in phenol-formaldehyde resins for particleboard production: I. Organosolv lignin modified resins," *Int. J. Adhes. Adhes.* 22(6), 481-486. DOI: 10.1016/S0143-7496(02)00059-3
- Del Saz-Orozco, B., Alonso, M. V., Oliet, M., Domínguez, J. C., and Rodriguez, F. (2015). "Mechanical, thermal and morphological characterization of cellulose fiber-reinforced phenolic foams," *Composites Part B* 75, 367-372. DOI: 10.1016/j.compositesb.2015.01.049
- Demirbas, A., Sahin-Demirbas, A., and Demirbas, A. H. (2004). "Turkey's natural gas, hydropower, and geothermal energy policies," *Energy Source* 26(3), 237-248. DOI: 10.1080/00908310490256590
- Ding, H., Wang, J., Liu, J., Xu, Y., Chen, R., Wang, C., and Chu, F. (2015). "Preparation and properties of a novel flame retardant polyurethane quasi-prepolymer for toughening phenolic foam," *J. Appl. Polym. Sci.* 132(35), 1-8. DOI: 10.1002/app.42424
- Doherty, W. O. S., Mousavioun, P., and Fellows, C. M. (2011). "Value-adding to cellulosic ethanol: Lignin polymers," *Ind. Crop. Prod.* 33(2), 259-276. DOI: 10.1016/j.indcrop.2010.10.022
- Dos-Santos, C. G., Costa, M. A., De Morais, W. A., and Pasa, V. D. (2010). "Phenolic foams from wood tar resols," *J. Appl. Polym. Sci.* 115(2), 923-927. DOI: 10.1002/app.30885
- El-Saied, H., Nada, A. M., Ibrahim, A. A., and Yousef, M. A. (1984). "Waste liquors from cellulosic industries. III. Lignin from soda-spent liquor as a component in phenol-formaldehyde resin," *Angew. Makromol. Chem.* 122(1), 169-181. DOI: 10.1002/apmc.1984.051220117

- El Hage, R., Brosse, N., Chrusciel, L., Sanchez, C., Sannigrahi, P., and Ragauskas, A. (2009). "Characterization of milled wood lignin and ethanol organosolv lignin from miscanthus," *Polym. Degrad. Stab.* 94(10), 1632-1638. DOI: 10.1016/j.polymdegradstab.2009.07.007
- Filley, T., Cody, G., Goodell, B., Jellison, J., Noser, C., and Ostrofsky, A. (2002). "Lignin demethylation and polysaccharide decomposition in spruce sapwood degraded by brown rot fungi," *Org. Geochem.* 33(2), 111-124. DOI: 10.1016/S0146-6380(01)00144-9
- Funaoka, M., Matsubara, M., Seki, N., and Fukatsu, S. (1995). "Conversion of native lignin to a highly phenolic functional polymer and its separation from lignocellulosics," *Biotechnol. Bioeng.* 46(6), 545-552. DOI: 10.1002/bit.260460607
- Gordobil, O., Egüés, I., Llano-Ponte, R., and Labidi, J. (2014). "Physicochemical properties of PLA lignin blends," *Polym. Degrad. Stabil.* 108, 330-338. DOI: 10.1016/j.polymdegradstab.2014.01.002
- Grishechko, L. I., Amaral-Labat, G., Szczurek, A., Fierro, V., Kuznetsov, B. N., and Celzard, A. (2013). "Lignin-phenol-formaldehyde aerogels and cryogels," *Micropor. Mesopor. Mat.* 168, 19-29. DOI: 10.1016/j.micromeso.2012.09.024
- GB/T 14074 (2006). "Testing methods for wood adhesives and their resins," Standardization Administration of China, Beijing, China.
- ISO 844 (2004). "Rigid cellular plastics – Determination of compression properties," International Organization for Standardization, Geneva, Switzerland.
- ISO 1209-1 (2004). "Rigid cellular plastics – Determination of flexural properties-Part 1: Basic bending test," International Organization for Standardization, Geneva, Switzerland.
- ISO 6187 (2001). "Rigid cellular plastics – Determination of friability," International Organization for Standardization, Geneva, Switzerland.
- Lee, W. J., Chang, K. C., and Tseng, I. M. (2012). "Properties of phenol-formaldehyde resins prepared from phenol-liquefied lignin," *J. Appl. Polym. Sci.* 124(6), 4782-4788. DOI: 10.1002/app.35539
- Li, X., Weng, J. K., and Chapple, C. (2008). "Improvement of biomass through lignin modification," *Plant. J.* 54(4), 569-581. DOI: 10.1111/j.1365-313X.2008.03457.x
- Liu, G. (1996). *Lignin Functional groups Analysis*, The Northeast Forestry University Press, Harbin.
- Ma, Y., Zhao, X., Chen, X., and Wang, Z. (2011). "An approach to improve the application of acid-insoluble lignin from rice hull in phenol-formaldehyde resin," *Colloids Surf. A* 377(1), 284-289. DOI: 10.1016/j.colsurfa.2011.01.006
- Ma, Y., Zhang, W., Wang, C., Xu, Y., and Chu, F. (2013). "The effect of formaldehyde/phenol (F/P) molar ratios on function and curing kinetics of high-solid resol phenolic resins," *J. Appl. Polym. Sci.* 129(6), 3096-3103. DOI: 10.1002/APP.38869
- Malutan, T., Nicu, R., and Popa, V. I. (2007). "Contribution to the study of hydroxymethylation reaction of alkali lignin," *BioResources* 3(1), 13-20. DOI: 10.15376/biores.3.1.13-20
- Mancera, C., Ferrando, F., Salvado, J., and El Mansouri, N. (2011). "Kraft lignin behavior during reaction in an alkaline medium," *Biomass Bioenergy* 35(5), 2072-2079. DOI: 10.1016/j.biombioe.2011.02.001
- Matsushita, Y., Wada, S., Fukushima, K., and Yasuda, S. (2006). "Surface characteristics of phenol-formaldehyde-lignin resin determined by contact angle measurement and

- inverse gas chromatography," *Ind. Crop. Prod.* 23(2), 115-121. DOI: 10.1016/j.indcrop.2005.04.004
- Matsushita, Y., Inomata, T., Hasegawa, T., and Fukushima, K. (2009). "Solubilization and functionalization of sulfuric acid lignin generated during bioethanol production from woody biomass," *Bioresour. Technol.* 100(2), 1024-1026. DOI: 10.1016/j.biortech.2008.07.026
- Pilato, L. (2013). "Phenolic resins: 100 years and still going strong," *React. Funct. Polym.* 73(2), 270-277. DOI: 10.1016/j.reactfunctpolym.2012.07.008
- Podschun, J., Saake, B., and Lehnens, R. (2015). "Reactivity enhancement of organosolv lignin by phenolation for improved bio-based thermosets," *Eur. Polym. J.* 67, 1-11. DOI: 10.1016/j.eurpolymj.2015.03.029
- Saisu, M., Sato, T., Watanabe, M., Adschari, T., and Arai, K. (2003). "Conversion of lignin with supercritical water-phenol mixtures," *Energ. Fuel.* 17, 922-928. DOI: 10.1021/ef0202844
- Tejado, A., Pena, C., Labidi, J., Echeverria, J., and Mondragon, I. (2007). "Physico-chemical characterization of lignins from different sources for use in phenol-formaldehyde resin synthesis," *Bioresour. Technol.* 98(8), 1655-1663. DOI: 10.1016/j.biortech.2006.05.042
- Wang, M., Leitch, M., and Xu, C. C. (2009). "Synthesis of phenol-formaldehyde resol resins using organosolv pine lignins," *Eur. Polym. J.* 45(12), 3380-3388. DOI: 10.1016/j.eurpolymj.2009.10.003
- Zhang, W., Ma, Y., Wang, C., Li, S., Zhang, M., and Chu, F. (2013a). "Preparation and properties of lignin-phenol-formaldehyde resins based on different biorefinery residues of agricultural biomass," *Ind. Crop. Prod.* 43(5), 326-333. DOI: 10.1016/j.indcrop.2012.07.037
- Zhang, W., Ma, Y., Xu, Y., Wang, C., and Chu, F. (2013b). "Lignocellulosic ethanol residue-based lignin-phenol-formaldehyde resin adhesive," *Int. J. Adhes. Adhes.* 40, 11-18. DOI: 10.1016/j.ijadhadh.2012.08.004
- Zhang, S., Dong, Q., Zhang, L., and Xiong, Y. (2016). "Effects of water washing and torrefaction on the pyrolysis behavior and kinetics of rice husk through TGA and Py-GC/MS," *Bioresour. Technol.* 199, 352-361. DOI: 10.1016/j.biortech.2015.08.110
- Zhao, M., Jing, J., Zhu, Y., Yang, X., Wang, X., and Wang, Z. (2016). "Preparation and performance of lignin-phenol-formaldehyde adhesives," *Int. J. Adhes. Adhes.* 64, 163-167. DOI: 10.1016/j.ijadhadh.2015.10.010
- Zhou, J., Hu, L., Liang, B., Bo, C., Jia, P., and Zhou, Y. (2015). "Preparation and characterization of novolac phenol-formaldehyde resins with enzymatic hydrolysis lignin," *J. Taiwan. Inst. Chem. E.* 54, 178-182. DOI: 10.1016/j.jtice.2015.03.023

Article submitted: October 11, 2016; Peer review completed: November 25, 2016;
Revised version received: December 1, 2016; Accepted: December 3, 2016; Published:
December 13, 2016.
DOI: 10.15376/biores.12.1.1015-1030